Interface amorphization in hexagonal boron nitride films on sapphire substrate grown by metalorganic vapor phase epitaxy

Xu Yang[1*], Shugo Nitta[2], Markus Pristovsek[2], Yuhuai Liu[2,3], Kentaro Nagamatsu[2], Maki Kushimoto[1], Yoshio Honda[2], and Hiroshi Amano[2,4,5]

[1]*Department of Electrical Engineering and Computer Science, Nagoya University, Nagoya 464-8603, Japan*

[2]*Institute of Materials and Systems for Sustainability, Nagoya University, Nagoya 464-8603, Japan*

[3]*School of Information Engineering, Zhengzhou University, Zhengzhou, 450001, China*

[4]*Akasaki Research Center, Nagoya University, Nagoya 464-8603, Japan*

[5]*Venture Business Laboratory, Nagoya University, Nagoya 464-8603, Japan*

E-mail: x_yang@echo.nuee.nagoya-u.ac.jp

Hexagonal boron nitride (h-BN) films directly grown on *c*-plane sapphire substrate by pulsed-mode metalorganic vapor phase epitaxy exhibit an interlayer for growth temperatures above 1200°C. Cross-sectional transmission electron microscopy shows that this interlayer is amorphous, while the crystalline h-BN layer above has a distinct orientation relationship to the sapphire substrate. Electron energy loss spectroscopy shows the energy-loss peaks of B and N in both amorphous interlayer and crystalline h-BN layer on top, while Al and O signals are also seen in the amorphous interlayer. Thus the interlayer forms during h-BN growth through decomposition of the sapphire at elevated temperatures.

Hexagonal boron nitride (h-BN) is a two-dimensional (2D) material like graphene and dichalcogenides. It is a promising material class for the development of future technologies.[1,2] h-BN has been investigated over the past years due to its extraordinary properties, such as wide bandgap,[3,4] high chemical and thermal stability,[5,6] electrical resistivity,[7] negative electron affinity,[8] large thermal neutron capture cross-section[9] and others. Unlike the conventional III-nitrides, its (0001) planes are nonpolar. Furthermore, p-type doping was reported with lower activation energy of the Mg acceptor compared with high Al-content AlGaN.[10] However, BN bulk crystal synthesized by traditional high pressure and high temperature methods is not ideal for future industrial demands because of the limited crystal size and 3D morphology. Furthermore, bulk crystal growth does not allow for thin functional layers or doping variations. To enable such applications, h-BN layers must been synthesized on large diameter foreign substrates with high crystalline quality and uniform morphology. While there are many reports of chemical vapor deposition of h-BN on transition metals, such as Cu,[11] Ru,[12] Pt[13] etc. These h-BN layers are usually limited in thickness to a few monolayers, and are then transferred to other substrates such as Si for further device fabrication. Direct synthesis of h-BN on micro-fabrication-compatible substrates like Si, SiC and α-Al_2O_3 would be preferable to avoid the complicated transfer process. Thus, there have been efforts to grow h-BN in metal-organic vapor phase epitaxy (MOVPE). For MOVPE, sapphire is one of most commonly used substrates due to its thermal stability and low costs. Kobayashi *et al.* reported that growth of h-BN by MOVPE with process temperature lower than 1100°C.[14,15] Li *et al.* investigated the growth of h-BN on sapphire using growth temperature of 1280°C.[16] The higher temperatures 1500°C or above have also been suggested and also reported for

synthesis of h-BN on sapphire wafer.[17,18] Among them, the smallest full-width at half-maximum in X-ray rocking curve for (0002) h-BN epitaxial layers was achieved by Jiang *et al*. on sapphire substrate.[19] Most of the previous studies reporting on the growth of h-BN on sapphire substrate focus on process condition effects and investigate the growth evolution from film surface. Reports on the structural evolution of h-BN grown on sapphire are scarce-especially at high temperature over 1200°C MOVPE growth, where sapphire degradation may occur and affect h-BN growth. In this work, we systematical studied the growth evolution of h-BN/sapphire interface and propose a temperature-related formation mechanism to account for an amorphous interlayer forming during h-BN overgrowth.

The BN films were grown on *c*-plane sapphire substrate by pulsed-mode MOVPE at growth pressure of 3.85 kPa over a range of growth temperature from 1030ºC to 1330ºC. Triethylboron (TEB) and ammonia (NH_3) diluted in hydrogen (H_2) gas were used as boron and nitrogen precursors, respectively. The supplied durations were 1 s for NH_3 and 2 s for TEB in each growth cycle, at different temperatures and time. Further details on the growth process are given in our previous paper.[20] The crystalline properties of grown BN layers were assessed by X-ray diffraction (XRD) using a five angle multi-crystal diffractometer. High resolution transmission electron microscopy (TEM) was measured on a Hitachi H-9500 microscope operating at 200 kV. TEM specimens were prepared by focused ion beam, and protective layers of Pt/C were deposited locally in the area of interest. Scanning transmission electron microscopy (STEM) and electron energy loss spectroscopy (EELS) were also performed operating at 200 kV.

Fig. 1(a) shows the 2θ-ω X-ray diffraction of a ~60-nm-thick h-BN layer grown on sapphire substrate at 1330°C. The (0002) h-BN reflection is clearly visible at ~26.4°,[9,21] and even the (0004) h-BN is observed at ~55.0°. Cross-sectional TEM images of the same layer along [11-20] zone axis are shown in Fig. 2(a). Two distinct layers with different structures are found in the epitaxial BN film. The upper layer close to the surface is a well-oriented layer, a stacking of highly ordered basal planes, i.e. crystalline h-BN layers. In contrast, the interlayer between the layered BN and sapphire substrate has no clearly ordered crystalline arrangement and no layered structure. This is further confirmed by electron diffraction patterns in Figs. 2(b) and (c). The top ordered layer (b) exhibits clearly resolved spots which indicates a hexagonal lattice arrangement in the top BN layer rather than turbostratic or amorphous. On the contrary, Fig. 2(c) shows a diffraction halo typical for the amorphous material, with only a faint hint of regular diffraction pattern. Thereby this interface layer (IF) consists of amorphous BN. This IF layer must have formed after the initial BN has been deposited, because the top h-BN has a rigid epitaxial relationship with the sapphire below.[20,22] This is further supported by TEM images of layers with different growth times from 5 min to 60 min at 1330°C. Figs. 3(a) and (b) show that there is only a very thin disordered IF layer after 5 min, while the amorphous thickness increases significantly after 30 min of growth. Further growth increases the IF layer thickness, as plotted in Fig. 3(c).

To understand the driving force for the formation of the amorphous IF layer, electron energy loss spectroscopy (EELS) was performed to probe the chemical composition and bonding structure in the BN film. EELS spectra were measured with a focused STEM probe at points along the growth direction from the amorphous interlayer to the upper h-

BN film. The EELS signal mainly originates from about 2 nm around the focal spot, and hence is sufficiently localized to distinguish the signal from individual layers. Both EELS spectra in the interface layer and the h-BN top layer in Figs. 4(a) and (b) show two distinct absorption features, one starting at 190 eV and the other at 401 eV. These correspond to the B *K* and N *K* edges.[23,24] The fine structure shows clear π* energy losses related to the transition of a 1s electron to the empty π* antibonding orbits. It is characteristic of sp^2–bonded BN.[25] Also, a series of σ* peaks are observable, corresponding to $1s \rightarrow \sigma^*$ transitions. This is consistent with h-BN. There are no obvious differences in the fine structures among the B *K* and N *K* peaks for the amorphous interlayer BN and topside h-BN layer, but the intensity ratio between π* and σ* differs between them. Hence significantly reduced h-BN unit in the amorphous layer compared with top BN layer. However, the interface layer also showed weak Al $L_{2,3}$ and O *K* signals, which are not detected in top h-BN film in Figs. 4(c) and (d). This indicates that the sapphire much have somewhat decomposed and diffused into the layer.

Since the amorphous layer only occurs at high growth temperatures, and it also contains Al and O, the interface amorphization is most likely associated with sapphire decomposition at high temperature. Sapphire degradation has been previously studied in literatures. Hexagonal pits were observed on sapphire surface after heating sapphire in H_2-containing gas ambient at 1065°C.[26] Degradation at higher temperatures is even more severe, especially *c*-plane sapphire decomposes strongly at temperatures exceeding 1200°C,[27] and even forming voids at an AlN/sapphire interface when annealing temperatures exceed 1300ºC.[28] Indeed, we observed an amorphous interface layer when the high temperature above 1200°C was sustained for more than 5 min. The extremely

low growth rate for h-BN (~1 nm/min) mandates long growth time and the top BN layer cannot protect sapphire. On the basis of these findings, it seems very reasonable that sapphire decomposition due to high temperature causes an amorphization of the h-BN layers on top, where the amorphous BN interface layer is formed by interdiffusion due to sapphire degradation at high temperatures. Whether it is via Al incorporation or rather the oxygen or simply due to a geometrical disruption is difficult to specify in this work. The critical temperature point to trigger the amorphization effect must be between 1030ºC to 1230ºC for our growth conditions, but would strongly depend on BN growth rate and growth conditions and other process parameters such as pressure, H_2/N_2 ratio in the carrier gas. For instance, sapphire annealed in He is able to withstand higher temperature as comparing to in H_2.[29] Since high temperature growth greatly improved the h-BN properties, more stable substrates than sapphire like AlN or SiC may an alternative ways to avoid the interface amorphization during h-BN growth. Indeed, as preliminary experiment of BN grown on AlN/sapphire template shows no amorphous interface layer even at 1330°C (Fig. 5). The thickness of layered h-BN was ~5 nm, and the growth conditions were the same as on the sapphire wafer.

In summary, well-orientated h-BN was grown on *c*-plane sapphire substrate by pulsed-mode MOVPE. At elevated temperatures, an unexpected amorphous BN interlayer was found at h-BN/sapphire interface. The interface amorphization consumed the h-BN from the sapphire interface. It is triggered by sapphire decomposition at high temperatures, in which the Al and O diffusion into the above h-BN, breaking h-BN lattice network and converting it to be disordered. Such interfacial layer does not form when growing h-BN on AlN/sapphire templates at high temperatures.

Acknowledgements

The author Xu Yang is an international research fellow of the Japan Society for the Promotion of Science (JSPS). This work is partially supported by JSPS KAKENHI #17J05229, National Institute for Materials Science, Strategic International Collaborative Research Program (SICORP) of Japan Science and Technology Agency (JST), JSPS and RFBR under Japan-Russia Research Cooperative Program, MOST-SKRDP (2016YFE0118400), and KPSTHP (172102410062).

References

1) C. R. Dean, A. F. Young, I. Meric, C. Lee, L. Wang, S. Sorgenfrei, K. Watanabe, T. Taniguchi, P. Kim, K. L. Shepard, and J. Hone, Nat. Nanotechnol. **5**, 722 (2010).
2) S. S. Wang, X. C. Wang, and J. H. Warner, ACS Nano **9**, 5246 (2015).
3) G. Cassabois, P. Valvin, and B. Gil, Nat. Photonics **10**, 262 (2016).
4) K. Watanabe, T. Taniguchi, and H. Kanda, Nat. Mater. **3**, 404 (2004).
5) L. H. Li, J. Cervenka, K. Watanabe, T. Taniguchi, and Y. Chen, ACS Nano **8**, 1457 (2014).
6) Z. Liu, Y. J. Gong, W. Zhou, L. L. Ma, J. J. Yu, J. C. Idrobo, J. Jung, A. H. McDonald, R. Vajtai, J. Lou and P. M. Ajayan, Nat. Commun. **4**, 2541 (2013).
7) L. G. Carpenter and P. J. Kirby, J. Phys. Appl. Phys. **15**, 1143 (1982).
8) R. W. Pryor, Appl. Phys. Lett. **68**, 1802 (1996).
9) J. Li, R. Dahal, S. Majety, J. Y. Lin, and H. X. Jiang, Nucl. Instrum. Meth. A. **654**, 417 (2011).
10) R. Dahal, J. Li, S. Majety, B. N. Pantha, X. K. Cao, J. Y. Lin, and H. X. Jiang, Appl. Phys. Lett. **98**, 21110 (2011).
11) K. K. Kim, A. Hsu, X. Jia, S. M. Kim, Y. Shi, M. Hofmann, D. Nezich, J. F. Rodriguez-Nieva, M. Dresselhaus, T. Palacios, and J. Kong, Nano Lett. **12**, 161 (2012).
12) P. Sutter, J. Lahiri, P. Zahl, B. Wang, and E. Sutter, Nano Lett. **13**, 276 (2013).
13) J.-H. Park, J. C. Park, S. J. Yun, H. Kim, D. H. Luong, S. M. Kim, S. H. Choi, W. Yang, J. Kong, K. K. Kim, and Y. H. Lee, ACS Nano **8**, 8520 (2014).
14) Y. Kobayashi, T. Akasaka, and T. Makimoto, J. Cryst. Growth **310**, 5048 (2008).
15) Y. Kobayashi and T. Akasaka, J. Cryst. Growth **310**, 5044 (2008).
16) X. Li, S. Sundaram, Y. El Gmili, T. Ayari, R. Puybaret, G. Patriarche, P. L. Voss, J. P. Salvestrini, and A. Ougazzaden, Cryst. Growth Des. **16**, 3409 (2016).
17) K. Nakamura, J. Electrochem. Soc. **133**, 1120 (1986).
18) T. Q. P. Vuong, G. Cassabois, P. Valvin, E. Rousseau, A. Summerfield, C. J. Mellor, Y. Cho, T. S. Cheng, J. D. Albar, L. Eaves, C. T. Foxon, P. H. Beton, S. V. Novikov, and B. Gil, 2D Mater. **4**, 021023 (2017).
19) H. X. Jiang and J. Y. Lin, Semicond. Sci. Technol. **29**, 084003 (2014).
20) X. Yang, S. Nitta, K. Nagamatsu, S.-Y. Bae, H.-J. Lee, Y. H. Liu, M. Pristovsek, Y.

Honda, and H. Amano, J. Cryst. Growth **482**, 1 (2018) .
21) S. Majety, J. Li, X. K. Cao, R. Dahal, B. N. Pantha, J. Y. Lin, and H. X. Jiang, Appl. Phys. Lett. **100**, 061121 (2012).
22) M. Snure, Q. Paduano, A. Kiefer, J. Cryst. Growth **436**, 16 (2016).
23) M. Wibbelt, H. Kohl, and P. Kohler-Redlich, Phys. Rev. B **59**, 11739 (1999).
24) R. Z. Ma, Y. Bando, T. Sato, and K. Kurashima, Chem. Mater. **13**, 2965 (2001).
25) Z.-G. Chen, J. Zou, G. Liu, F. Li, Y. Wang, L. Wang, X.-L. Yuan, T. Sekiguchi, H.- M. Cheng, and G. Q. Lu, ACS Nano **2**, 2183 (2008).
26) J. Tajima, Y. Kubota, R. Togashi, H. Murakami, Y. Kumagai, and A. Koukitu, Phys. Status Solidi C **5**, 1515 (2008).
27) K. Nomura, S. Hanagata, A. Kunisaki, R. Togashi, H. Murakami, Y. Kumagai, and A. Koukitu, Jpn. J. Appl. Phys. **52**, 08JB10 (2013).
28) Y. Kumagai, Y. Enatsu, M. Ishizuki, Y. Kubota, J. Tajima, T. Nagashima, H. Murakami, K. Takada, and A. Koukitu, J. Cryst. Growth **312**, 2530 (2010).
29) K. Akiyama, T. Araki, H. Murakami, Y. Kumagai, and A. Koukitu, Phys. Status Solidi C **4**, 2297 (2007).

List of figures

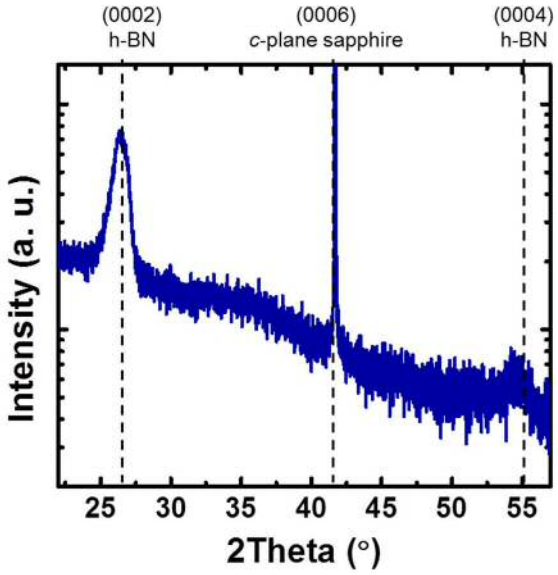

Fig. 1

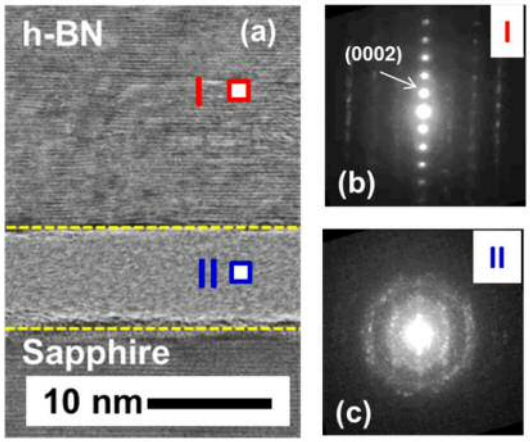

Fig. 2

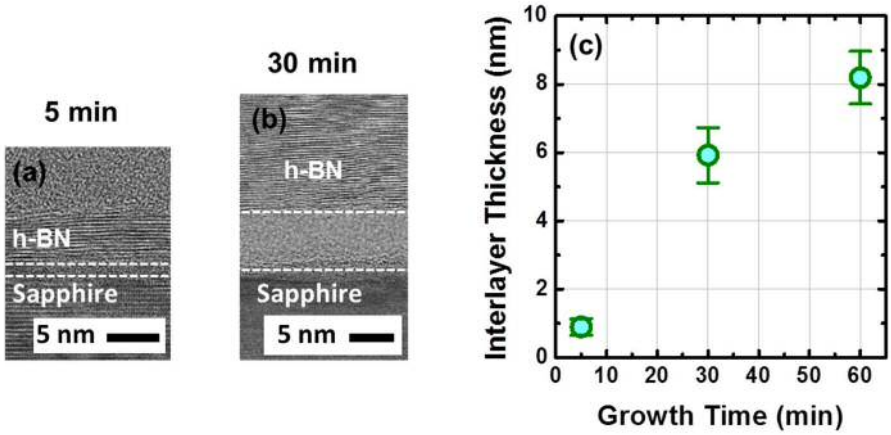
5 min
(a)
h-BN
Sapphire
5 nm
30 min
(b)
h-BN
Sapphire
5 nm
(c)
Interlayer Thickness (nm)
Growth Time (min)
0
2
4
6
8
10
0
10
20
30
40
50
60

Fig. 3

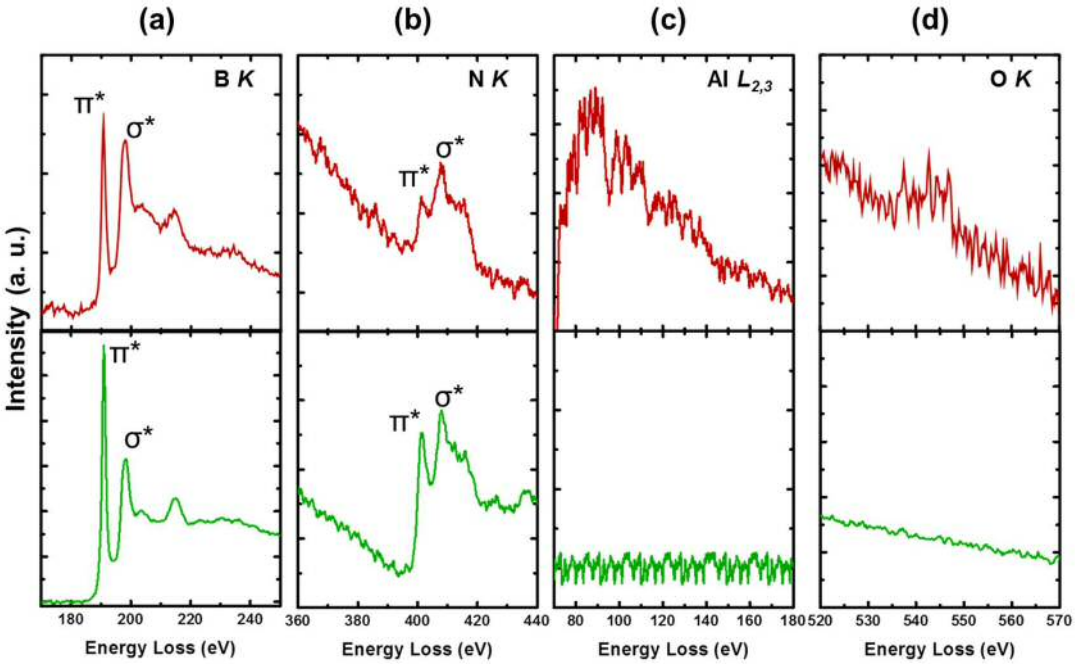
(a)
(b)
(c)
(d)
B K
N K
Al L2,3
O K
π*
σ*
Intensity (a. u.)
Energy Loss (eV)
180
200
220
240
360
380
400
420
440
80
100
120
140
160
180
520
530
540
550
560
570

Fig. 4

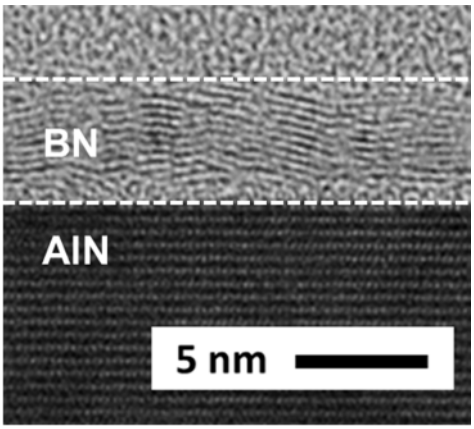

Fig. 5

Figure Captions

Fig. 1 XRD 2θ-ω scan of ~60-nm-thick h-BN on sapphire grown at 1330°C.

Fig. 2 (a) Cross-sectional STEM image of ~60 nm thick h-BN on sapphire grown at 1330°C. (b) and (c) are diffraction patterns for the selected area I and II.

Fig. 3 Cross-sectional TEM images of h-BN grown on sapphire grown at 1330°C. (a) Growth time is 5 min. (b) Growth time is 30 min. (c) Interlayer thickness versus growth time for BN films grown on sapphire.

Fig. 4 EELS spectra of amorphous interlayer (red) and layered BN on the topside (green) of ~60 nm thick h-BN film grown at 1330°C.

Fig. 5 Cross-sectional TEM image of ~5 nm thick h-BN grown at T_g =1330°C on an AlN/sapphire template.